CHINESE JOURNAL OF PHYSICS VOL. 52, NO. 1-II February 2014

Review

Fragmentation of Hydrocarbon Molecules in Intense Laser Fields Studied by Coincidence Momentum Imaging: a Review

Bosi Yang,[1] Li Zhang,[2,*] Huailiang Xu,[1,3,4,†] Ruxin Li,[3,‡] and Kaoru Yamanouchi[4,§]

[1] *State Key Laboratory on Integrated Optoelectronics, College of Electronic Science and Engineering, Jilin University, Changchun 130012, China*

[2] *Communications and Electronic Information Department, Shanghai Vocational College of Science and Technology, Shanghai 201800, China*

[3] *State Key Laboratory of High Field Laser Physics, Shanghai Institute of Optics and Fine Mechanics, Chinese Academy of Sciences, Shanghai, 201800, China*

[4] *Department of Chemistry, School of Science, The University of Tokyo, 7-3-1 Hongo, Bunkyo-ku, Tokyo, 113-0033, Japan*

(Received August 30, 2013)

Fragmentation of polyatomic molecules is a fundamental chemical reaction in intense laser fields when the electric field strength of the laser pulse is comparable to or exceeds the intramolecular Coulomb binding fields. For hydrocarbon molecules, because of the migration of light hydrogen atom (or proton) that can lead to chemical bond rearrangement of molecules, fragmentation of hydrocarbon molecules may result in new fragment species that could not be realized from the initial geometry of molecules by direct bond breaking, making the full characterization of their dynamical fragmentation processes difficult. In this article, we will review recent progress in the study of fragmentation of hydrocarbon molecules induced by intense laser fields using the coincidence momentum imaging method that can provide definite information on the fragmentation channels of molecules. The effect of hydrogen migration on fragmentation of hydrocarbon molecules is reviewed, based on which new possible schemes for controlling chemical bond breaking/formation by controlling the motion of protons within a hydrocarbon molecule is discussed.

DOI: 10.6122/CJP.52.652 PACS numbers: 82.50.Nd, 42.65.Re, 33.15.Ta

I. INTRODUCTION

Innovative progress of ultrashort laser technology in the last three decades has enabled to generate intense laser fields whose electric field strength is comparable to or even exceeds that of the Coulomb binding field within atoms and molecules [1]. Exposed to such intense laser fields, polyatomic molecules have been found to exhibit a variety of characteristic dy-

*Electronic address: zhangli19833@126.com
†Electronic address: huailiang@jlu.edu.cn
‡Electronic address: ruxinli@mail.shcnc.ac.cn
§Electronic address: kaoru@chem.s.u-tokyo.ac.jp

 © 2014 THE PHYSICAL SOCIETY OF THE REPUBLIC OF CHINA

namical processes such as field alignment [2], molecular orientation [3], stabilization [4], enhanced ionization [5, 6], and dissociation [7]. In particular, fragmentation of multi-charged polyatomic molecules in intense laser fields [1, 8–15], in which molecules undergo rapid bond breaking by "Coulomb explosion" due to intra-molecular Coulombic repulsive forces between the positively charged constituents in the highly charged parent ion, is one of such fundamental dynamical processes. Since the Coulomb explosion occurs very rapidly, the resultant fragmented ions would carry valuable information on instantaneous geometrical structure of the parent molecule just before the Coulomb explosion, providing direct access to the investigation on the structural deformation of molecules induced by laser irradiation [16, 17]. Thus, fragmentation of polyatomic molecules via Coulomb explosion has been an attractive research field in the last decade both experimentally and theoretically [18].

A recently developed experimental method called coincidence momentum imaging (CMI) [16], which allows the determination of the full momentum vectors of all the fragmented ions ejected from a single parent molecular ion in an ultrashort intense laser field, provides the possibility to snapshot the molecular structure just before Coulomb explosion in intense laser fields. The CMI method employs a multi-hit position sensitive detector (PSD), which offers two major advantages over the previous momentum imaging methods such as the mass-resolved momentum imaging [19, 20] and the covariance mapping [10]. First, all the fragment ions originating from a single parent ion are identified in coincidence so that the charge number of the parent ions as well as its dissociation pathways can be specified definitively. Second, the three-dimensional (3D) momentum vectors of respective fragment ions are determined in the laboratory frame for every single event of the Coulomb explosion. For example, for hydrocarbon molecules, it was reported by using CMI method that di- and tri-atomic hydrogen molecular ions can be ejected from alcohol molecules in an intense, short-pulse laser field [21, 22], which revealed that the fragmentation of hydrocarbon molecules via Coulomb explosion is generally accompanied by remarkably fast hydrogen and/or proton migration from one site to another within a molecule.

Due to the large mobility of hydrogen atom or proton, ultrafast intra-molecular processes of hydrogen migration can lead to large-scale deformation of molecular skeletal structure and rearrangement of chemical bonds, and thus often determine the main reaction routes of fragmentation by suppressing other competing processes [23]. Especially fragmentation of hydrocarbon molecules may result in new fragment species that could not be realized from the initial geometry of molecules by direct bond breaking, which makes hydrogen migration one of the most important molecular rearrangement processes in various chemical reactions [24, 25] as well as in strong laser field phenomena [13, 26, 27].

So far, a series of intensive studies of laser-induced hydrocarbon molecular fragmentation via Coulomb explosion has been investigated by the CMI method, which aimed to explore more details about the ultrafast dynamics of molecules and to control the molecular bond-breaking and bond-creation behaviors in chemical reactions induced by intense laser fields. Indeed, impressive study progress in the fragmentation of hydrocarbon molecules induced by intense laser fields has been made by using the CMI method, which includes different species of hydrocarbon molecules such as alkanes (e.g. acetonitrile [26, 28]), alkenes including olefin (e.g. ethylene [29], allene [27, 30, 31]) and diolefins (e.g. 1,3-

butadiene [29, 32–35]), alkynes (e.g. acetylene [36, 37] and methyl acetylene [38, 39]), alcohol (e.g. methanol [22, 40–44] and ethanol [29]) and aromatic hydrocarbon such as benzene [45]. Identification of the fragmentation channels from two-body [26, 28, 30, 38, 40, 43, 44, 46], three-body [27, 34, 36, 41, 44], four-body [37], even complete Coulomb explosion process [34] has been successfully realized. Furthermore, based on the correlations of the fragment momentum vectors determined by the CMI method, identification of the fragmentation of a specific channel occurring in a sequential or a concerted manner can also be realized [35, 41].

By using the CMI method, the fragmentation of hydrocarbon molecules accompanied with the hydrogen atom (or proton) migration has been studied as well [28], which revealed that, taking the triply charged 1,3-butadiene for example, not only one proton but two protons can migrate in intense laser fields [34]. It was also shown that the intense laser field can induce two distinctively different stages of the hydrogen migration in hydrocarbon molecules, that is the hydrogen migration occurring within the laser pulse and the post-pulse hydrogen migration process [47]. In addition, the competition between the hydrogen-atom migration and the Coulomb explosion during the fragmentation in intense laser fields was studied [48, 49]. It is worth of stressing that isomerization of acetylene to vinylidene has been extensively studied as a prototype of hydrogen migration in intense laser fields by different methods [23, 46, 50–53].

Since one of the major goals in modern photochemistry is to control photo-induced chemical reactions by designing light pulses, the effects of parameters of ultrashort laser pulses such as intensity [35], pulse duration [54], polarization state [35] and wavelength [54] on the fragmentation of hydrocarbon molecules in intense laser fields have also been investigated. Control of hydrocarbon molecular fragmentation channels on sub-fs time scale via optical waveform controlled laser field was realized [55]. Recently, the effects of laser parameters on ultrafast hydrogen migration in the fragmentation of methanol have been systematically studied as well [56], in order to show the feasibility for controlling chemical bond formation as well as chemical bond breaking by controlling the motion of hydrogen atoms (or protons) within a hydrocarbon molecule.

Therefore, the purpose of this article is to review recent progress in the study of fragmentation of hydrocarbon molecules induced by intense laser fields using the CMI method, which can provide definite information on the ultrafast fragmentation dynamics of molecules. The article is organized as following: In Section II we will briefly introduce the CMI method, which shows itself as a versatile tool for investigating ultrafast molecular reaction dynamics. Section III we will give an overview of the recent achievements in the study of fragmentation of hydrocarbon molecules via Coulomb explosion CMI method. In Section IV real-time visualizing ultrafast fragmentation dynamics of hydrocarbon molecules by the pump-probe Coulomb explosion CMI method will be presented. In Section V a short summary is given.

II. COINCIDENCE MOMENTUM IMAGING

The CMI method has been growing in popularity and sophistication over the last 20 years [57–66], and was first introduced for studying the decomposition processes of molecules in intense laser fields in 2001 [16]. In the CMI method, all the fragment ions produced from a single parent molecular ion are detected in coincidence using a PSD, allowing a secure assignment of the fragmentation pathways. In addition, the momentum vectors of the respective fragment ions ejected by a single Coulomb explosion event are determined in the laboratory frame, from which detailed information on the geometrical structure of a parent ion at the instance of the Coulomb explosion can be obtained. It has been demonstrated in the previous studies that the CMI method is an ideal approach to investigate, at a single molecular level, the fragmentation dynamical processes of polyatomic molecules including the ultrafast hydrogen migration dynamics in an intense laser field.

A typical CMI apparatus is shown in Fig. 1 [16]. Intense laser fields in laser-molecule interaction region were generated by focusing ultrashort femtosecond laser pulses (e.g. from a femtosecond Ti: Sapphire Chirped Pulse Amplification (CPA) laser system) onto the crossing point of a sample molecular beam at right angles in an ultrahigh vacuum chamber (up to 10^{-11} mbar). The density of the molecular beam was controlled so that the number of ionized molecules per laser pulse becomes less than one unity. The laser polarization direction was set to be parallel to the detector plane.

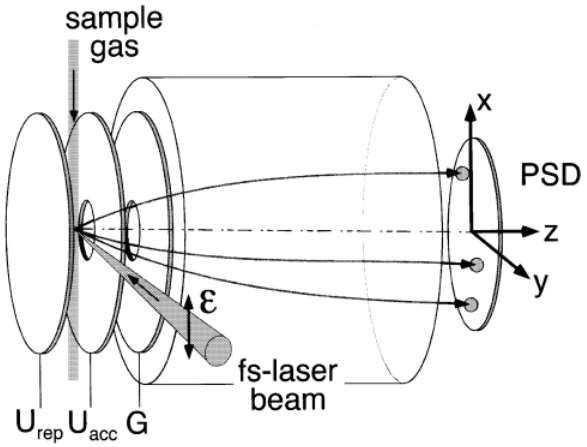

FIG. 1: A typical CMI experimental apparatus (Adapted from [16]).

The laser produced ions or electrons in the intersection area can be extracted by a three-electrode electrostatic lens to a Position Sensitive Detector (PSD) with delay-line anodes [61]. The three-electrode electrostatic lens is composed of three equally spaced (d = 15 mm) parallel plate electrodes, which are defined as repeller, accelerator and ground electrodes. The electrodes are 0.2-mm-thick stainless steel plates with a 70 mm diameter. The repeller electrodes contain a small hole $\sim$ 1–2 mm, which passes through the on-axis

molecular beam, and the accelerator and ground electrodes are with a 20-mm diameter hole in the velocity mapping configuration to avoid the blurring effect on the ion images, which could occur when mesh grids are employed. Ions produced by the laser excitation are first pushed away by the repeller plate, and then accelerated after passing the accelerator plate toward the open ground electrode. And then the ions enter a time-of-flight (TOF) tube between the ground electrodes and the detector, which is a vacuum enclosure, free of electrical fields, and usually referred to "field free drift region". The voltages applied to the repeller and the accelerator plates can be adjusted to achieve optimized conditions of the ion images.

After passing through the TOF tube, the charged particles are detected by a position-sensitive microchannel plate (MCP) detector with delay-line-anode readouts, which can realize acquisition of the signals from the hardware modules and recording of data event-by-event to PCs for further online/offline data analysis. The delay-line anode also benefits in many aspects, such as allowing the detection for much higher rates in MHz, achieving high position and time resolution and extending the capability to handle multiple hits in nanosecond time intervals. The signals on each end of the anodes generated from the respective fragment ions generated by an event of the Coulomb explosion of a single parent molecule are amplified and discriminated, and then processed to a time-to-digital converter, based on which the (x, y) positions on the PSD and the time of flight, T, of the respective ions can be obtained. The position resolution of the MCP delay-line detector can be less than 0.1 mm, and the MCP multi-hit dead time is about 10-20 ns. Therefore the MCP detector with delay-line-anode can provide high resolution of three-dimensional imaging and timing information for charged particles detection at high rates with multi-hit capability.

The 3D momentum vector, $p = (p_x, p_y, p_z)$, of a single fragmented ion at its birth can be retrieved by its recorded position (x, y) on the detector plane and its time-of-flight, T [16]. The two momentum components, p_x and p_y, along the x- and y-axes in the laboratory frame (see Fig. 1) are expressed as

$$p_x = m\Delta x/T, \tag{1}$$

$$p_y = m\Delta y/T, \tag{2}$$

with m being the mass of the ion, and $(\Delta x, \Delta y)$ the displacements of the fragment ion from the position where the ion with $p_x = p_y = 0$ would hit. The momentum component p_z along the z-axis is expressed as

$$p_z = \{\alpha q \cdot (U_{rep} - U_{acc})/d\} \cdot (T_0 - T) \tag{3}$$

where q is the charge of the ion, T_0 is the arrival time of fragment ion with $p_z = 0$, and U_{rep} and U_{acc} are the electric potentials at the repeller and accelerator plate electrodes, respectively. The correction factor α is introduced for compensating a weak inhomogeneity of the electric field in the repeller and accelerator region.

The spectrometer in the CMI technique can also be used to project ions and electrons onto oppositely positioned detectors equipped at the two ends of the spectrometer, as shown in Fig. 2.

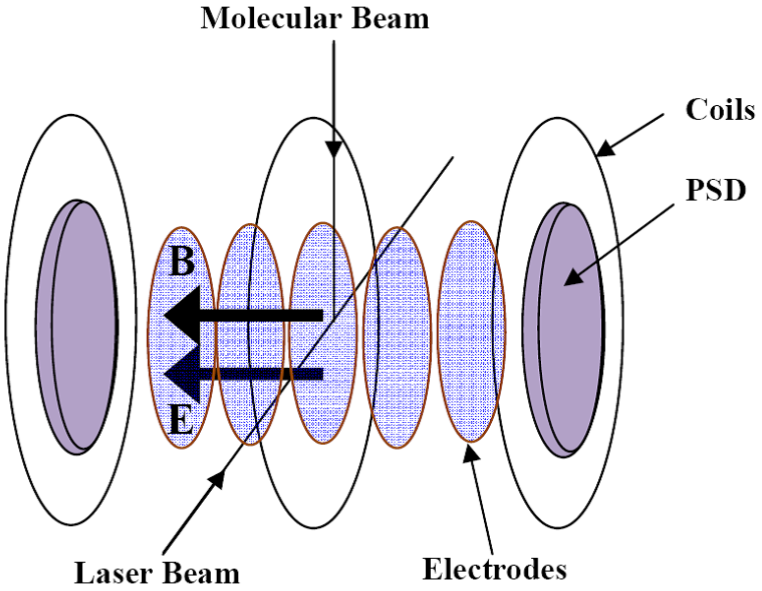

FIG. 2: A typical CMI apparatus for photon-electron and photon-ion detection.

Here we will briefly give the forms of the 3D momentum vector, $p = (p_x, p_y, p_z)$, for both ions and electrons recorded by the CMI technique with a uniform electrostatic field and a uniform magnetic field applied to the spectrometer [62–64]. Supposing the Cartesian lab-coordinate system is defined as following: the direction of the cold gas jet is along the x axis, the direction of the laser beam propagation is along the y axis and the electrostatic field direction is along the z axis.

The initial three momentum components of the ith ion from a single parent molecular ion, $p^i = (p_x^i, p_y^i, p_z^i)$, in the laboratory frame can be expressed as

$$p_x^i = m_i \Delta x / T, \tag{4}$$

$$p_y^i = m_i \Delta y / T, \tag{5}$$

$$p_z^i = m_i l_a / T - (1/2) q_i E_s T, \tag{6}$$

where m_i and q_i are the mass and the charge of the ion from a single parent molecule respectively, and Δx, Δy are the displacements of the fragment ion from the position where the ion with $p_x = p_y = 0$ would hit, T is the time-of-flight of the ion from the reaction volume to the detector, l_a is the travelling distance of the ion in the z-axis direction, and E_s is the magnitude of the uniform electrostatic field of the spectrometer.

The initial three momentum components of electron, $p^e = (p_x^e, p_y^e, p_z^e)$, in the laboratory frame can be expressed as

$$p_x^e = \{eB/(2\sin(\alpha/2))\}\{-x \cdot \cos(\alpha/2) + y \cdot \sin(\alpha/2)\}, \tag{7}$$

$$p_y^e = \{eB/(2\sin(\alpha/2))\}\{x \cdot \sin(\alpha/2) + y \cdot \cos(\alpha/2)\}, \tag{8}$$

$$p_z^e = m_e l_a/T - (1/2)eE_sT, \tag{9}$$

where m_e and e are the mass and the charge of the electron respectively, and B is the magnitude of the uniform magnetic field. α depends on the ratio of the time-of-flight to the electron orbital period T with the following relation

$$\alpha = \mod(T, T_0) \times 360^\circ, \tag{10}$$

where $T_0 = 2\pi m_e/eB$. For details of expressions of the full momentum vectors for both ions and electrons in the CMI technique, the readers are referred to Ref. [60].

III. FRAGMENTATION OF HYDROCARBON MOLECULES IN INTENSE LASER FIELDS STUDIED BY CMI

Fragmentation reactions of polyatomic molecules are essential building blocks of chemistry. Earlier investigations on fragmentation of triatomic molecules such as CO_2 [19] and CS_2 [20] in intense laser fields have unveiled the large deformation of their skeletal structure along both the bending and the stretching coordinates. Since the CMI technique was successfully applied to strong field physics and chemistry for studying the decomposition processes of molecules [16], intensive studies of fragmentation dynamical processes of hydrocarbon molecules have been carried out, which pushes forwards a lot on current understanding of strong field laser-induced molecular dynamics. In this section, we will give an overview of the recent (after the year 2000) achievements in the study of fragmentation dynamics of different hydrocarbon molecules by the Coulomb explosion CMI method, which includes the identification of the fragmentation channels, molecular structural deformation, the ejection of di- and tri-hydrogen molecular ions, the ultrafast hydrogen migration dynamics, the sequential versus concerted fragmentation dynamics, and control of molecular fragmentation dynamics via laser pulse parameters and intra-molecular hydrogen migration process. The reason why hydrocarbon molecules were paid much attention is due to ultrafast hydrogen migration which may proceed when hydrocarbon molecules are exposed to intense laser fields and makes the full characterization of fragmentation dynamics complicated. It would be very meaningful to get a more detailed insight into the fascinating ultrafast hydrogen migration phenomena that may contribute to controlling laser-induced chemical bond breaking and formation in photo-chemistry.

III-1. Identification of molecular fragmentation channels

By using the CMI method as introduced previously, the position and the time of flight of each detected charged particle can be measured, based on which the 3D momentum vector of the particle can be deduced. To identify a specific fragmentation channel of a molecule from the multi-body Coulomb explosion, the momentum of electrons can be

neglected because the momentum imposed on an emitted electron is more than two orders of magnitude smaller than that of the fragment ions. Therefore, according to the momentum conservation conditions in all three spatial dimensions, a particular fragmentation channel of molecules decomposed from one particular charge state of interest can be uniquely identified by selecting only sets of fragment ions whose sum-momentum $P_s = p_s^i$ fulfills $|P_s| = 0$, where p_s^i ($s = x$, y, z in the laboratory frame) denotes the momentum of the ith fragment ion produced from a single parent ion along the s-axis. As a result false coincidence events originating from more than two parent ions in the interaction region were excluded based on the momentum vectors of all the fragment ions from a single parent ion detected in coincidence.

By using the CMI method, two-body Coulomb explosions of acetylene [46], acetonitrile (CH_3CN) and deuterated acetonitrile (CD_3CN) [26, 28], methanol (CH_3OH) [22, 40, 42, 44] and its isotopomers (CD_3OH, CH_3OD) [40, 42, 43], allene [30], 1,3-butadiene [32], methylacetylene (CH_3CCH) and its isotopomer methyl-d3-acetylene (CD_3CCH) [38] in intense laser field have been investigated and the corresponding two-body Coulomb explosion fragmentation channels have been identified. Three-body Coulomb explosion fragmentations of methanol-d (CH_3OD^{3+}) [41], acetylene [36, 37], methanol [44], allene [27, 31], 1,3-butadiene [33, 35], acetylene [36], methylacetylene (CH_3CCH) and its isotopomer methyl-d3-acetylene (CD_3CCH) [39] in intense laser field have also been identified. Four-body Coulomb explosion fragmentation channels of acetylene [37] and even complete Coulomb explosion of highly charged 1,3-butadiene ($CH_2CHCHCH_2$) [34, 67] and methane (CH_4) molecules [67] in intense laser fields have been identified as well. In the later study of complete Coulomb explosion of molecule, it was very interesting that the energetic protons could be ejected from a concerted Coulomb explosion from unexpectedly high charge states of polyatomic hydrocarbon molecules induced by intense laser fields [34]. The observations were explained by the enhanced ionization taking place at many C-H bonds simultaneously. The occurrence of enhanced ionization of hydrocarbon molecules was also observed in dissociative double ionization of formic acid by intense 100 fs laser pulses at 800 nm using ion–ion coincidence momentum spectroscopy [68].

III-2. Molecular structural deformation

With the identification of the fragmentation channels of a molecule, the fragmentation dynamics with interest can be discussed based on the momentum correlations of the involved fragment ions as they provide a deeper understanding on the molecular structural deformation. In early measurement using the CMI technique, the molecular geometrical structure of CS_2^{3+} just before the Coulomb explosion of $CS_2^{3+} \rightarrow S^+ + C^+ + S^+$, was constructed straightforwardly from the momentum correlations of the three fragment ions, which exhibited that the C-S bond length and the S-C-S bond angle vary rapidly in the laser fields, revealing the skeletal structural deformation of CS_2 (see Fig. 3) [16]. Subsequent investigation of structural deformation of hydrocarbon molecules induced by intense laser fields was carried out by the CMI method.

In the investigation of the two-body Coulomb explosions of acetonitrile, $CH_3CN^{2+} \rightarrow CH_{3-n}^+ + H_nCN^+$ ($n = 0$–2), and of deuterated acetonitrile, $CD_3CN^{2+} \rightarrow CD_{3-n}^+ + D_nCN^+$

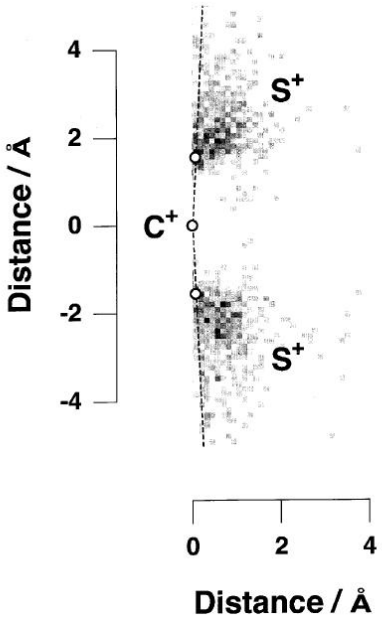

FIG. 3: The reconstructed geometrial structure of CS_2^{3+} just before the three-body Coulomb explosion of $CS_2^{3+} \rightarrow S^+ + C^+ + S^+$ (Adapted from [16]).

(n = 0–2), in intense laser fields (0.15 PW/cm^2, 70 fs) by the CMI method [26, 28], it was found that the doubly charged parent molecules undergo the substantial structural deformation in intense laser fields along the C–C–N bending coordinate prior to the two body explosion. The two-body Coulomb explosion of allene (CH_2CCH_2) induced by an ultrashort ($\sim$ 40 fs) intense laser field by the CMI method [30] reported that structural deformation of the C-C-C skeleton was expected to occur by the migration of the hydrogen atom in C_3H_4 based on the fragmentation channels of $C_3H_4^{2+} \rightarrow CH^+ + C_2H_3^+$ and $C_3H_4^{2+} \rightarrow CH_3^+ + C_2H^+$. However, by the two-body Coulomb explosion, it is difficult to obtain the information on how large the structural deformation proceeds.

The three-body Coulomb explosion of hydrocarbon molecules was also used to study the structural deformation by using the triple-ion CMI method [27, 33]. From the momentum correlation maps, the geometrical structures of triply charged allene [27] and 1,3-butadiene [33] were shown. In particular, it was recently revealed that the molecular structural deformation to non-planar geometry can be identified by the time-resolved four-body Coulomb explosion CMI, highly charged deuterated acetylene ($C_2D_2^{4+}$) [37].

III-3. Ejection of di- and tri-atomic hydrogen molecular ions

The ejection of hydrogen molecular ions, H_2^+ and H_3^+ is a noteworthy dynamical process in the fragmentation of hydrocarbon molecules in intense laser fields because it may reflect the ultrafast intramolecular dynamics of hydrogen atoms in hydrocarbon molecules. By using the CMI method, formation of H^+, H_2^+ and H_3^+ was confirmed from the ion ejection

through two-body coulomb explosions of $CH_3OH^{2+} \rightarrow H_n^+ + COH_{4-n}^+$ ($n = 1$–3) of doubly charged methanol [22], and the lifetimes of the corresponding precursor ions CH_3OH^{2+} are estimated to be 70–290 fs for the H^+ ejection, 110–550 fs for the H_2^+ ejection, and a much longer value than 1.4 ps for the H_3^+ ejection.

The ejection of hydrogen molecular ions from two-body Coulomb explosion processes of methanol (CH_3OH) and its isotopomers (CD_3OH and CH_3OD) was also systematically studied by using the CMI method in order to clarify ultrafast dynamics of hydrogen atoms in hydrocarbon molecules in intense laser field [42]. In this study, the ejection hydrogen molecular ions through the fragmentation channels of $CH_3OH^{2+} \rightarrow H_m^+ + CH_{(3-m)}OH^+$ ($m = 2, 3$), $CD_3OH^{2+} \rightarrow D_m^+ + CD_{(3-m)}OH^+$ ($m = 2, 3$) and $CH_3OD^{2+} \rightarrow H_m^+ + CH_{(3-m)}OD^+$ ($m = 2, 3$) were identified. In addition, the ejections of H/D exchanged hydrogen molecular ions (HD^+, HD_2^+ and H_2D^+) were observed, and the timescales for the H/D exchanging processes were also estimated from the extent of anisotropy in the ejection directions [42]. Formation of H^+, H_2^+ and H_3^+ through two-body Coulomb explosion of other hydrocarbon molecules such as allene has also been identified, as shown in Fig. 4.

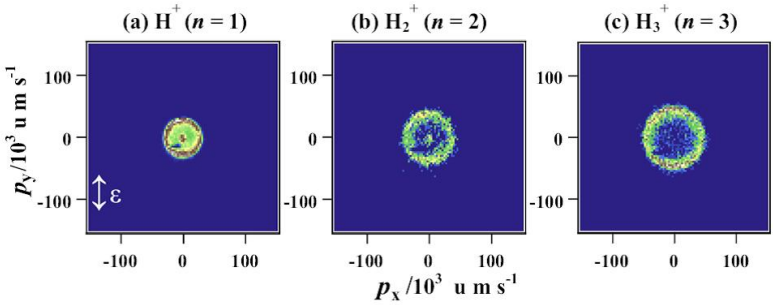

FIG. 4: Observed two-dimensional coincidence momentum maps of (a) H^+, (b) H_2^+, and (c) H_3^+ produced through the two-body Coulomb explosion processes of $C_3H_4^{2+}$. (Adapted from [30].)

Furthermore, ejections of H^+ and H_2^+ ions from three-body fragmentation channels of triply charged methanol and methanol-d through $CH_3OH^{3+} \rightarrow H^+ + H_2^+ + COH^+$ and $CH_3OD^{3+} \rightarrow H^+ + H_2^+ + COD^+$ induced by an ultrashort intense laser field was investigated [41], in which it was identified for the first time that there are two types of sequential pathways: one is a pathway in which H^+ is ejected first and the other is a pathway in which H_2^+ is ejected first.

III-4. Ultrafast hydrogen migration

The hydrogen migration process, in which hydrogen atom(s) or proton(s) migrates from one site to another within a molecule, can lead to large-scale deformation of molecular skeletal structure and chemical bond rearrangement, and thus may result in reaction channels that could not be realized when reactions start from the initial molecular geometries [26]. Investigations of fragmentation of polyatomic molecules in intense laser fields by the CMI method have revealed the existence of ultrafast hydrogen migration in a series of hydrocarbon molecules [52, 73].

Two-body Coulomb explosion of acetonitrile (CH_3CN) and deuterated acetonitrile (CD_3CN), in intense laser fields (0.15 PW/cm^2, 70 fs) was reported in 2004 by the CMI method, in order to clarify the hydrogen migration process occurring simultaneously with the abrupt C-C bond breaking [26, 28]. Three different explosion pathways for the respective species, i.e., $CH_3CN^{2+} \rightarrow CH_{3-n}^{+} + H_nCN^{+}$ (n = 0–2) and $CD_3CN^{2+} \rightarrow CD_{3-n}^{+} + D_nCN^{+}$ (n = 0–2), were securely identified, and the migration of hydrogen atom (or proton) from CH_3 moiety to the CN moiety was readily identified by detecting HCN^{+} or H_2CN^{+} fragments ions because all the three hydrogen atoms belong initially to the terminal carbon atom. It was found that the fragment anisotropy becomes more isotropic as n increases from 0 to 2, showing that the rate of the Coulomb explosion becomes comparable with or even longer than the rotational period of the parent molecule as the migration of hydrogen atoms from the methyl group to the nitrile group proceeds.

To give a deeper understanding of the hydrogen migration, the dissociation pathways with hydrogen/deuterium migration or hydrogen/deuterium exchange have been investigated [38–40]. It was shown on methanol (CH_3OH, CD_3OH, CH_3OD) that hydrogen/deuterium migration or hydrogen/ deuterium exchange prior to the C-O bond breaking in an intense laser field (0.2 PW/cm^2, 60 fs) was securely confirmed by the CMI method [40]. From the anisotropic angular distributions and the relative yields of the fragment ions, it was revealed that the hydrogen migration process was terminated within the period of an intense ultrashort laser pulse. A comparison of the results obtained from CH_3OH and those from its isotopomers showed that the hydrogen migration was decelerated by the isotope substitution. By studying the two-body Coulomb explosion of methanol by the CMI method, pulse duration effect on the hydrogen migration has also been explored. In comparison of hydrogen migration pathway and non-hydrogen migration pathway of methanol with the C-O bond breaking obtained with the pulse durations [43], it was shown that when the pulse duration becomes longer, the major ionization mechanism for both the direct and the migration pathways changes from the nonsequential ionization to the sequential ionization and the hydrogen migration occurs more efficiently.

The two-body and three-body break-up channels involving association and migration of hydrogen atoms during the fragmentation of methanol dication were also investigated via the CMI technique to further study how the hydrogen atom migrates during a sequential breakup fragmentation channel [44]. Three-body associative break-ups were found to occur sequentially, triggered by the loss of one hydrogen atom, followed by separation of charges. Based on the fragment momentum distributions it was proposed that hydrogen atom migration was induced in the first stage of the sequential breakup.

The isomerization between acetylene (HCCH) and vinylidene (H_2CC) via hydrogen migration has been extensively studied as a prototype of hydrogen migration [8, 14–22, 36, 46]. The angle between the momenta of C^{+} and H^{+} fragments exhibited a sharp distribution peaked at a small angle ($\sim 20^{\circ}$) when ultrashort ($\sim$ 9 fs) laser pulses was applied, showing that the hydrogen atom remained near the original carbon site in the acetylene configuration. However a significantly broad distribution extending to larger momentum angles ($\sim 120^{\circ}$) was observed when the pulse duration was increased to 35 fs, indicating that the ultrafast isomerization to vinylidene was induced in the longer laser

pulse.

Ultrafast hydrogen migration in allene (CH_2=C=CH_2) in intense laser fields was also investigated by the CMI method [27, 30, 31]. Two types of two-body Coulomb explosion pathways, $C_3H_4^{2+} \rightarrow CH_m^+ + C_2H_{4-m}^+$ (m = 1–3) and $C_3H_4^{2+} \rightarrow C_3H_{4-n}^+ + H_n^+$ (n = 1–3), were securely identified. The formation of CH_3^+, $C_2H_3^+$, and H_3^+ showed that the chemical bond rearrangement associated with the ultrafast hydrogen migration occurs and that the extent of the hydrogen migration determines either one of the two initially identical C=C chemical bonds was broken [30]. By the combination of the momentum correlation maps and the geometrical structure of triply charged allene reconstructed from the observed momentum vectors of fragment ions, the migrating proton covering the entire range of an allene molecule was visualized, as shown in Fig. 5 [27]. The extent of hydrogen migration was also found to play a decisive role in breaking selectively one of the two initially equivalent C–C chemical bonds that become inequivalent in the course of the hydrogen migration. Moreover it was further shown that the decomposition of highly charged allene ion via three-body Coulomb explosion proceeds in a stepwise manner as well as in a concerted manner, and the time scale of the hydrogen migration within allene was estimated to be $\sim$ 20 fs [31].

The existence of ultrafast hydrogen atom migration was also found in 1,3-butadiene (H_2C=CH-CH=CH_2) in intense laser fields using the CMI method [32, 33]. In the two-body dissociation processes of doubly charged 1,3-butadiene, the existence of the two dissociation pathways, $C_4H_6^{2+} \rightarrow CH_3^+ + C_3H_3^+$ and $C_4H_6^{2+} \rightarrow C_2H_2^+ + C_2H_4^+$, can be regarded as evidences of the chemical bond rearrangement processes associated with hydrogen migration in the intense laser field. It was found that the hydrogen atom bonded originally to one of the two central carbon atoms migrates preferentially to its neighboring terminal carbon atom site [32, 33]. The spatial distribution maps of a migrating proton reconstructed for the two three-body Coulomb explosion pathways, $C_4H_6^{3+} \rightarrow H^+ + CH_3^+ + C_3H_2^+$ and $C_4H_6^{3+} \rightarrow H^+ + C_2H^+ + C_2H_4^+$, revealed that two protons migrate within a 1,3-butadiene molecule, prior to the three-body decomposition [33]. Two-proton migration process was also found in the two-body decomposition processes of methylacetylene (CH_3CCH) and its isotopomer methyl-d_3-acetylene (CD_3CCH) in intense laser fields (790 nm, 40 fs, 5.0×10^{13} W cm^{-2}). It was revealed from the analysis of the CMI data that the migration of two deuterons as well as the exchange between a proton and a deuteron occurs prior to the two-body decomposition of a doubly charged parent molecule [38].

Hydrogen and deuteron migration processes were further investigated in the three-body Coulomb explosion processes of triply charged ions of methylacetylene (CH_3-C≡C-H) and its isotopomer, methyl-d_3-acetylene (CD_3-C≡C-H), induced by an ultrashort intense laser field (790 nm, $\sim$ 40 fs, 5.0×10^{13} W cm^{-2}), from the observed momentum vectors of all the three fragment ions for each decomposition pathway and the proton and deuteron distributions constructed in the coordinate space [39]. It was shown that the hydrogen migration proceeds more efficiently from the methyl group than from the methane group. In addition to the decomposition pathways accompanying the migration of one H (or D) atom, the decomposition pathways accompanying the migration of two light atoms (H/D exchange and 2D migration) were identified. Furthermore, the decomposition pathways ascribable to

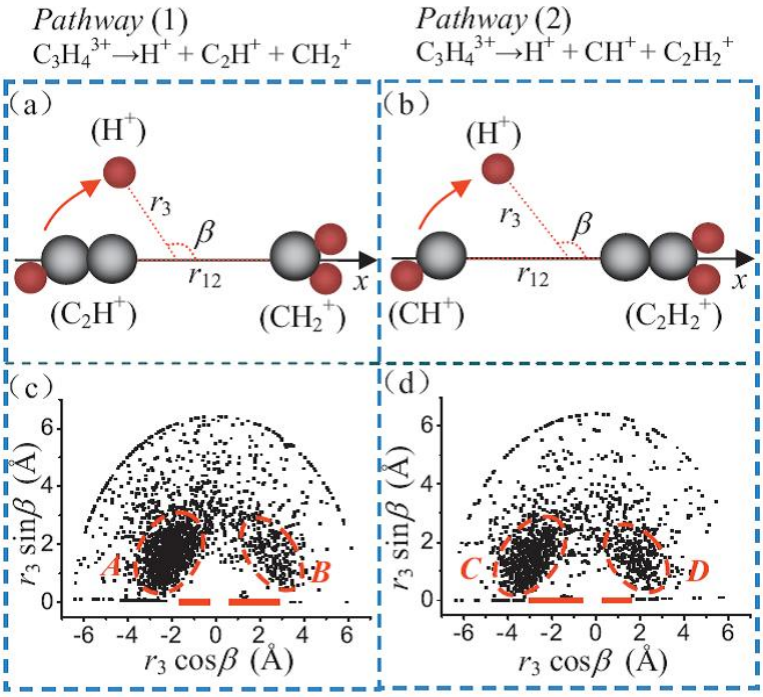

FIG. 5: The geometrical structure of $C_3H_4^{3+}$ constructed from the observed momentum vectors of the respective fragment ions ejected through the Coulomb explosion of *Pathway* (1): $C_3H_4^{3+} \rightarrow H^+ + C_2H^+ + CH_2^+$ (left) and *Pathway* (2): $C_3H_4^{3+} \rightarrow H^+ + CH^+ + C_2H_2^+$ (right). The two red horizontal bars represent the ranges of the position of the charge centers of the two heavy moieties (Adapted from [27]).

the migration of three light atoms (H/D exchange followed by D migration) were identified, showing the high intramolecular mobilities of H and D atoms within methylacetylene and methyl-d3-acetylene in an intense laser field, resulting in the H/D scrambling.

III-5. Sequential versus concerted fragmentation dynamics

Using the CMI method, it was possible to elucidate how the Coulomb explosion actually proceeds, whether in a concerted manner or in a sequential manner. The first investigation using CMI technique to explore this issue was successfully carried out for CS_2^{3+} in intense laser fields [17] where the formation of a sequential explosion of CS_2^{3+} prior to the complete three-body fragmentation was unveiled. Similar investigations were subsequently carried out on hydrocarbon molecules.

The three-body Coulomb explosion of triply charged methanol-*d* (CH_3OD^{3+}) through $CH_3OD^{3+} \rightarrow H^+ + H_2^+ + COD^+$ induced by a laser field of $\sim 2 \times 10^{14}$ W/cm^2 was investigated by the CMI method [41], in which it was identified that the explosion proceeds in a stepwise manner with two types of sequential pathways: one is the pathway in which H^+ is ejected first, and the other is the pathway in which H_2^+ is ejected first. It was revealed from

the CMI data that when H^+ is ejected first the broad distribution of H^+ ejection direction indicates that the torque is efficiently imposed on CH_2OD^{2+} for the rotational excitation, and/or the lifetime of CH_2OD^{2+} is longer than the rotational period of CH_2OD^{2+}; however when the H_2^+ is ejected first the narrow distribution of H_2^+ ejection angle suggested not large enough torque on $CHOD^{2+}$ at the first-step decomposition for the efficient rotational excitation of the $CHOD^{2+}$. The narrow distribution was also considered to come from the shorter lifetime of $CHOD^{2+}$.

Three-body associative break-ups of methanol dication were found to occur sequentially, triggered by the loss of one hydrogen atom, followed by separation of charges [44].

The analysis of the fragment momentum correlations in the fragmentation of deuterated benzene (C_6D_6) in ultrashort intense laser fields (9 fs, 1×10^{15} W/cm^2) by the CMI method revealed that all the observed three-body explosion processes proceed sequentially via the formation of molecular dications $C_mD_n^{2+}$, with (m, n) = (6,5), (5,5), (5,4), (4,4), (4,3), and (3,3) as precursors, which further dissociate into pairs of monocations [45].

The three-body Coulomb explosion of allene (CH_2=C=CH_2) induced by ultrafast intense laser fields was also analyzed to investigate the fragmentation dynamics by the Coulomb explosion CMI method [31]. On the basis of the kinetic energy distributions of the fragment ions produced through the two three-body Coulomb explosion pathways, $C_3H_4^{3+} \rightarrow H^+ + CH^+ + C_2H_2^+$ and $C_3H_4^{3+} \rightarrow H^+ + C_2H^+ + CH_2^+$, as well as the proton maps of both pathways, it was shown that the decomposition proceeds in a stepwise manner as well as in a concerted manner. Whether the proton ejection proceeds concertedly or sequentially was also studied for triply charged 1,3-butadiene molecules through examining the three-body fragmentation of $C_4H_6^{3+}$ [35].

Field ionization and Coulomb explosion of very highly charged hydrocarbon molecules, methane (CH_4) and 1,3-butadiene (C_4H_6), driven by intense laser pulses were studied in a combined theoretical framework and the experimental CMI method [67]. It was demonstrated that the high degree of ionization leads to the complete Coulomb explosion of the molecules, and the Coulomb explosion in the studied molecular systems is a sudden, all-at-once fragmentation where the ionization step is followed by a simultaneous ejection of the charged fragments. In this case protons are ejected simultaneously in a concerted process.

III-6. Control of molecular fragmentation dynamics

Controlling of chemical reaction dynamics of hydrocarbon molecules with different methods, such as chirped intense laser fields [69], the pulse width and wavelength [54], the intensity [35] and polarization state of the laser pulse [35], the shaped intense few-cycle laser pulses [55, 70–72] and so forth, have been carried out. Recently the effect of hydrogen migration on fragmentation of hydrocarbon molecules has also been investigated. The hydrogen migration process can lead to large-scale deformation of molecular skeletal structure and chemical bond rearrangement, and thus may open new reaction pathways that could not be realized when reactions start from the initial molecular geometries [47, 52, 73]. Here we will only focus on recent works of controlling fragmentation dynamics of hydrocarbon molecules studied by using the CMI method.

Using the CMI method, the effect of the pulse duration of intense laser fields on hydrogen migration dynamics in methanol was examined, where two-body Coulomb explosion channels with the C–O bond breaking of methanol induced by ultrashort intense laser fields whose pulse durations are $\Delta t = 7$ and 21 fs respectively, were investigated [43]. When $\Delta t = 7$ fs, the angular distribution of recoil vectors of the fragment ions for the hydrogen migration pathway of $CH_3OH^{2+} \rightarrow CH_2^+ + H_2O^+$, in which one hydrogen migrates from the carbon site to the oxygen site prior to the C–O bond breaking, exhibits a peak deflected from the laser polarization direction by 30°–45°. When the laser pulse duration was stretched to $\Delta t = 21$ fs, the angular distributions for the migration pathways exhibit a broad peak along the laser polarization direction which is probably due to the dynamical alignment and/or the change in the double ionization mechanism; that is, from the nonsequential double ionization to the sequential double ionization. It was also shown that the stretch of the laser pulse duration from 7 fs to 21 fs does not influence the momentum distribution, suggesting that $\Delta t = 21$ fs is not long enough for the C-O bond distance to be elongated so that the enhanced ionization proceeds. However when a pulse with pulse duration of $\Delta t = 60$ fs [40] was used, it is found that the $\Delta t = 60$ fs pulse is sufficiently long for the C-O bond distance to become stretched so that the major ionization mechanism changes to the enhanced ionization. Therefore changing the pulse duration may lead to the ionization process occurring in different mechanism, thus makes it possible to control the ejection directions and the momentum distributions of the fragment ions produced through the hydrogen migration pathway.

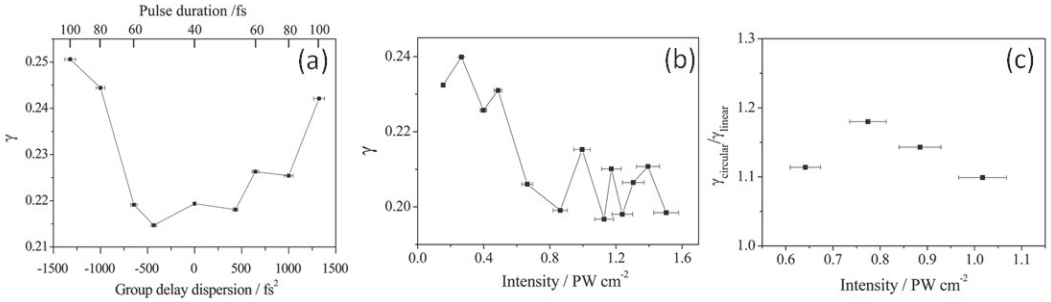

FIG. 6: The ratio γ of the yield obtained for the migration pathway of $CH_3OH^{2+} \rightarrow CH_2^+ + OH_2^+$ with respect to the sum of the yields of the migration pathway and the nonmigration pathway of $CH_3OH^{2+} \rightarrow CH_3^+ + OH^+$ as a function of the laser pulse duration and the intensity are shown in (a) and (b) respectively. The ratio of γ obtained with the circularly polarized light ($\gamma_{circular}$) with respect to γ obtained with linearly polarized light (γ_{linear}) at four different laser peak intensities of the linearly polarized pulses is shown in (c) (Adapted from [56]).

The effect of laser parameters (intensity, duration, and polarization) of ultrashort laser pulses (795 nm, 40–100 fs, and 0.15–1.5 $\times$ 10^{15} W/cm^2) on the ultrafast hydrogen migration in methanol was systematically investigated using the Coulomb explosion CMI technique. It was reported that the ratio of the ion yield γ obtained for the migration pathway $CH_3OH^{2+} \rightarrow CH_2^+ + OH_2^+$ with respect to the sum of the yields obtained for the

migration pathway and for the nonmigration pathway $CH_3OH^{2+} \rightarrow CH_3^+ + OH^+$ exhibits a small but clear dependence on laser pulse properties. It was found that the yield ratio becomes larger by a factor of $\sim 20\%$ when the laser pulse duration increases from 40 to 100 fs, as can be seen in Fig. 6(a) [56]. However the ratio becomes smaller by $\sim 17\%$ when the laser intensity increases from 0.15×10^{15} to 1.5×10^{15} W/cm^2 (see Fig. 6(b)). It was also found that the ratio of the hydrogen migration is enhanced by 10–18% in a circularly polarized laser field as compared to that in a linearly polarized laser field with the same laser peak intensity, as shown in Fig. 6(c).

The dependence of the fragmentation dynamics of 1,3-butadiene on the intensity and polarization state of the laser pulse was also investigated by the CMI technique [35]. It was found that both the relative probability of fragmenting via a certain path and the probability of hydrogen migration prior to the Coulomb explosion depend on the two varied laser pulse parameters, intensity and polarization, as can be seen in Fig. 7.

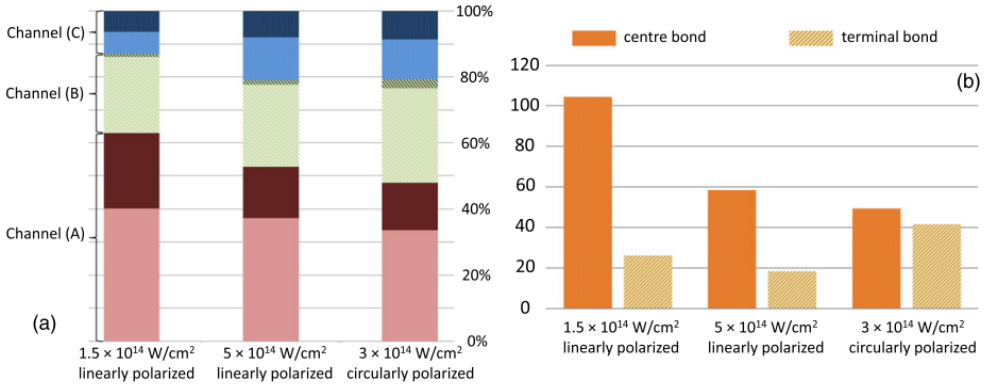

FIG. 7: (a) Event numbers of the two dominant paths of channels (A)–(C) normalized to the sum of events for all three channels as a function of pulse intensity and laser polarization state, i.e. channel (A): $H^+ + C_2H_2^+ + C_2H_3^+$, full red; channel (B): $H^+ + CH_3^+ + C_3H_2^+$, dashed green; channel (C): $H^+ + CH_2^+ + C_3H_3^+$, dotted blue. (b) Ratio of bond breaking events of doubly charged 1,3-butadiene involving hydrogen-atom migration normalized to the number of counts where the same bond is broken without hydrogen-atom migration as a function of pulse intensity and laser polarization state. The columns denoted with *centre bond* correspond to the ratio of events in the two fragmentation channels: $C_4H_6^{2+} \rightarrow C_2H_3^+ + C_2H_3^+$ and $C_4H_6^{2+} \rightarrow C_2H_2^+ + C_2H_4^+$ respectively, the columns denoted with *terminal bond* correspond to the two fragmentation channels: $C_4H_6^{2+} \rightarrow CH_3^+ + C_3H_3^+$ and $C_4H_6^{2+} \rightarrow CH_2^+ + C_3H_4^+$ respectively (Adapted from [35]).

Control over various fragmentation reactions of a series of hydrocarbon molecules (acetylene, ethylene, 1,3-butadiene) by the optical waveform-controlled intense few-cycle laser pulses was also demonstrated experimentally by using the CMI method [55]. A strong carrier-envelope phase (CEP) dependence on the fragmentation yields obtained from different fragmentation channels of all the three hydrocarbon molecules was found, as can be seen in Figs. 8(a)–(c). The intensity dependence on the ion yield was also demonstrated, as seen Figs. 8(d)–(f). It was proposed that the responsible mechanism behind is inelastic ionization

from inner-valence molecular orbits by recolliding electron wave packets, whose recollision energy in few-cycle ionizing laser pulses strongly depends on the optical waveform. This work demonstrated an efficient and selective way of predetermining fragmentation reaction in hydrocarbon molecules on sub-femtosecond time scales.

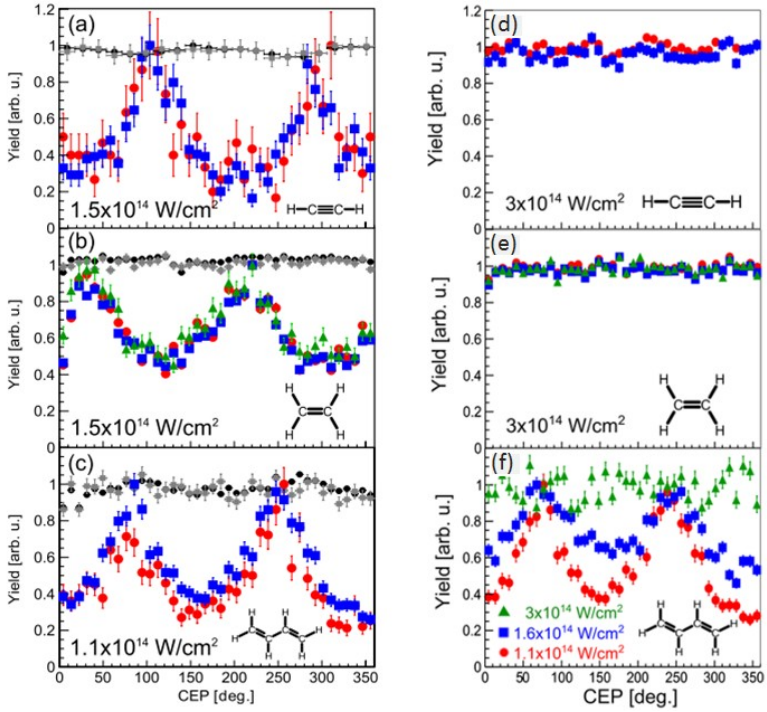

FIG. 8: (a)–(c) Measured fragmentation and ionization yields, normalized to 1 at their respective maxima, as a function of CEP for different fragmentation channels of acetylene (a), ethylene (b), and 1,3-butadiene (c), measured at the laser intensities indicated in the panels. The various fragmentation reactions are $C_2H_2^{2+} \rightarrow CH^+ + CH^+$ (red dots) and $C_2H_2^{2+} \rightarrow H^+ + C_2H^+$ (blue squares) for acetylene in (a); $C_2H_4^{2+} \rightarrow CH_2^+ + CH_2^+$ (red dots), $C_2H_4^{2+} \rightarrow H^+ + C_2H_3^+$ (blue squares), and $C_2H_4^{2+} \rightarrow C_2H_2^+ + H_2^+$ (green triangles) for ethylene in (b); $C_4H_6^{2+} \rightarrow C_2H_3^+ + C_2H_3^+$ (red dots) and $C_4H_6^{2+} \rightarrow CH_3^+ + C_3H_3^+$ (blue squares) for 1,3-butadiene in (c). The ionization yields of the singly and doubly charged molecular ions are denoted by black dots and gray squares, respectively. (d), (e) Fragmentation yields over the CEP of the same channels as in (a) and (b) (same color and point styles apply), but measured for a slightly higher intensity (as indicated). (f) Measured intensity dependence of the yield of the fragmentation channel $C_4H_6^{2+} \rightarrow CH_3^+ + C_3H_3^+$ over CEP. The intensities are indicated in the figure (Adapted from [55]).

IV. REAL-TIME VISUALIZING ULTRAFAST DYNAMICS OF HYDROCARBON MOLECULES BY PUMP-PROBE COULOMB EXPLOSION CMI METHODS

So far tracing/visualizing the ultrafast dynamics such as hydrogen migration during molecular fragmentation processes in real time has become one of the most attractive challenges in ultrafast molecular science. Investigations on this subject have been carried out by the pump-probe Coulomb explosion CMI methods for hydrocarbon molecules [47, 52].

It was demonstrated in 2007 that the visualization of ultrafast hydrogen migration in deuterated acetylene dication ($C_2D_2^{2+}$) was achieved in real time by employing the pump-probe Coulomb explosion imaging with sub-10-fs intense laser pulses (9 fs, 0.13 PW/cm^2, 800 nm) [52]. The pump laser pulses were used to doubly ionize the deuterated acetylene as well as to trigger the hydrogen migration. The probe laser pulses with a time delay Δt relative to the pump pulses were then applied to ionize $C_2D_2^{2+}$ to $C_2D_2^{3+}$ and to probe the structural change of $C_2D_2^{2+}$. The instantaneous location of the migrating deuterium atom between the two carbon sites, $DCCD^{2+} \leftrightarrow D_2CC^{2+}$, was identified from the momenta of fragment ions in the three-body Coulomb explosion process through $C_2D_2^{3+} \rightarrow D^+ + C^+ + CD^+$. It was shown from the temporal evolution of the momenta of the fragment ions produced from this three-body Coulomb explosion that the migration proceeds in a recurrent manner: the deuterium atom first shifts from one carbon site to the other in a short time scale ($\sim$ 40 fs) and then migrates back to the original carbon site by 280 fs, as can be seen in Fig. 9, in competition with the molecular dissociation.

Using the pump-probe CMI method, hydrogen migration in methanol induced by an intense laser field (0.2 PW/cm^2) was also investigated in real time [47]. Singly charged molecular ions, $(CH_3 \cdots OH)^+$ and $(CH_2 \cdots OH_2)^+$, which was prepared by the pump pulses are further ionized by the probe pulse into doubly charged molecular ions, $CH_3^+ \cdots OH^+$ and $CH_2^+ \cdots OH_2^+$, leading to the two-body Coulomb explosion, respectively. One fragmentation channel produces CH_3^+ and OH^+ without hydrogen migration, and the other generates CH_2^+ and OH_2^+ through a hydrogen atom migration.

The yields of the two Coulomb explosion channels of $CH_3OH^{2+} \rightarrow CH_3^+ + OH^+$ and $CH_3OH^{2+} \rightarrow CH_2^+ + OH_2^+$ and the obtained sum of the kinetic energy released from a pair of the fragment ions, E_{kin}, as functions of the relative delay Δt between the pump and probe pulses are shown in Figs. 10(a) and (b). It was observed that the peak position of the kinetic energy distributions for the lower strip with $E_{kin} \leq 3.8$ eV in both pathways shifts toward lower energies when Δt increases. The time-dependent lower strips in Figs. 10(a) and (b) reflect the temporal evolution of a dissociating wave packet of $(CH_3 \cdots OH)^+$ and that of $(CH_2 \cdots OH_2)^+$, respectively. Thus the distance between CH_3^+ and OH^+ through the nonmigration pathway, and that between CH_2^+ and OH_2^+ through the migration pathway from the two-body Coulomb explosion processes, can be estimated as a function of the delay time, as can be seen in Figs. 10(a) and (b). The yield ratios of the nonmigrated and migrated species $\eta_{non-mig}$ and η_{mig} for the lower strips shown in Figs. 10(a) and 10(b) exhibit clear temporal change: as the time delay increases, $\eta_{non-mig}$ decreases, but η_{mig} increases, showing that the hydrogen migration proceeds even after molecules interact with the intense laser field. The time constant for this post-laser pulse hydrogen migration

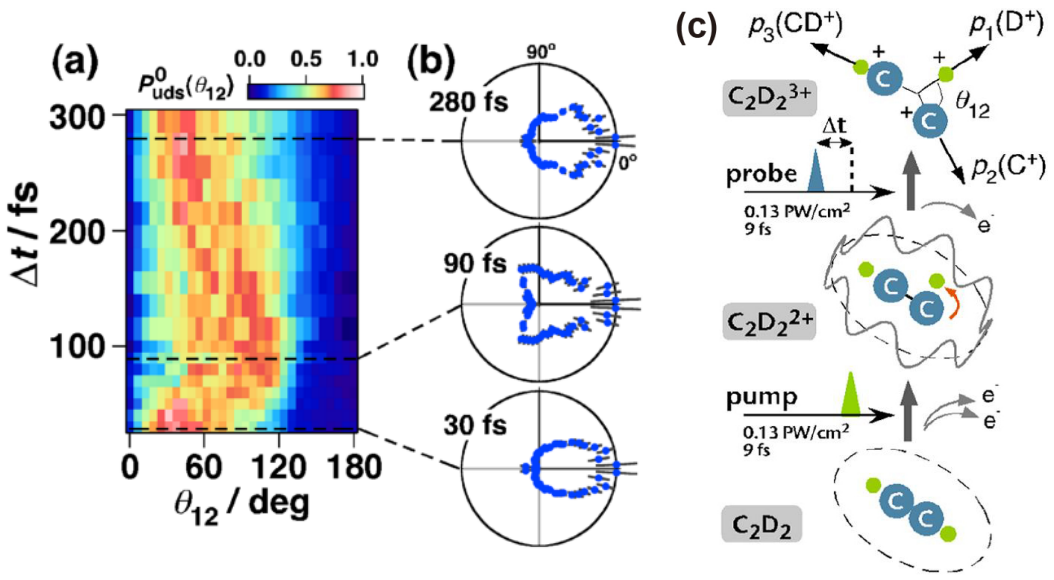

FIG. 9: (a) Evolution of θ_{12} (as presented in (c)) recorded in steps of 10 fs for $\Delta t \leq 100$ fs and 20 fs for $\Delta t > 100$ fs, showing that the deuterium atom rapidly migrates from one carbon site to the other within 90 fs and then migrates back to the acetylene configuration in 280 fs. (b) The $\theta_{12}/\sin(\theta_{12})$ distributions at three selected time delays, $\Delta t = 30$, 90, and 280 fs, expressed in the polar plot. (c) The concept diagram of the pump-probe Coulomb explosion imaging (Adapted from [52]).

was evaluated to be $\sim$ 150 fs. In addition, the ejection of the fragment ions through the migration pathway shown in the upper strip with $E_{kin} > 3.8$ eV indicates the existence of the hydrogen migration occurring with the laser pulse. Thus, this work revealed that the intense laser fields can induce two distinctively different hydrogen migration processes, that is, ultrafast hydrogen migration occurring within the intense laser field and slower post laser pulse hydrogen migration.

The visualization of ultrafast isomerization of deuterated acetylene dication ($C_2D_2^{2+}$) was also demonstrated by time-resolved Coulomb explosion imaging with sub-10 fs intense laser pulses (9 fs, 0.13 PW/cm^2, 800 nm). The Coulomb explosion imaging monitoring the three-body explosion process, $C_2D_2^{3+} \rightarrow D^+ + C^+ + CD^+$, as a function of the delay between the pump and probe pulses revealed that the migration of a deuterium atom proceeds in a recurrent manner: one of the deuterium atoms first shifts from one carbon site to the other in a short timescale ($\sim$ 90 fs), and then migrates back to the original carbon site by 280 fs, in competition with the molecular dissociation. Correlated motions of the two deuterium atoms associated with the hydrogen migration and structural deformation to non-planar geometry were also identified by the time-resolved four-body Coulomb explosion imaging, $C_2D_2^{4+} \rightarrow D^+ + C^+ + C^+ + D^+$ [37].

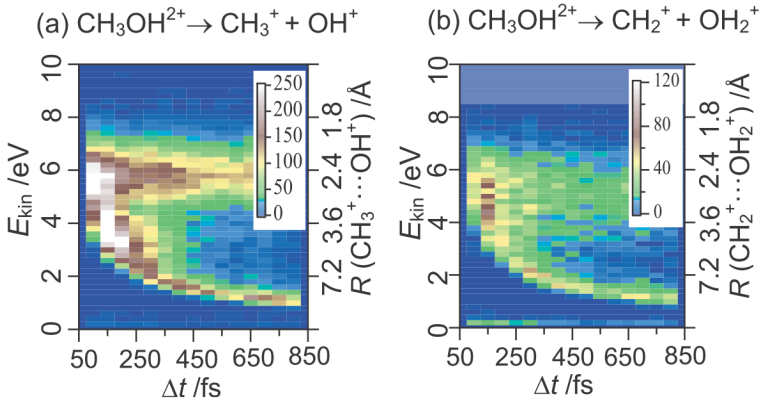

FIG. 10: The E_{kin}-Δt 2D contour plots for the yield distributions of the fragment ions ejected through (a) $CH_3OH^{2+} \rightarrow CH_3^+ + OH^+$ and (b) $CH_3OH^{2+} \rightarrow CH_2^+ + OH_2^+$, where E_{kin} is the kinetic energy released from a pair of fragment ions (a) [CH_3^+, OH^+], and (b) [CH_2^+, OH_2^+], and R is the distance between the two fragment ions in each pathway (Adapted from [52]).

V. SUMMARY

In this article, we reviewed the fragmentation of hydrocarbon molecules in intense laser fields studied by the CMI method. Since in the hydrocarbon molecules, the dynamics of hydrogen atoms (or protons) takes place on a timescale that is in between the one of the sub-femtosecond motion of electrons and the one of the other moieties, which due to their much bigger mass are by at least an order of magnitude slower, leading to a much more complicated reactions when hydrocarbon molecules are exposed to intense laser fields. The CMI method has been proved to be a powerful tool for characterizing the fragmentation dynamics of chemical reaction of molecules at a single molecule level. Using the Coulomb explosion CMI method, various types of fragmentation processes associated with the hydrogen migration processes in hydrocarbon molecules in intense laser fields were identified, and it was found that hydrogen atom or proton plays an important role in the chemical bond formation and breaking reaction. By introducing recent achievements in the study of fragmentation of hydrocarbon molecules by using Coulomb explosion CMI method, as well as real-time visualizing ultrafast fragmentation dynamics of hydrocarbon molecules by the pump-probe Coulomb explosion CMI method, we expect that this article could provide a more detailed insight into chemical reactions of hydrocarbons in intense laser field as well as new prospects for efficient coherent reaction control with tailored laser pulses.

Acknowledgement

This work is financially supported by National Natural Science Foundation of China (Grant Nos. 11074098, 61235003 and 61308030), the Open Fund of the State Key Laboratory of High Field Laser Physics (SIOM), the Fundamental Research Funds of Jilin University, and JSPS short-term fellowship program.

References

[1] K. Yamanouchi, Science **295**, 1659 (2002).
[2] H. Stapelfeldt and T. Seideman, Rev. Mod. Phys. **75**, 543 (2003).
[3] J. J. Larsen, K. Hald, N. Bjerre, H. Stapelfeldt, and T. Seideman, Phys. Rev. Lett. **85**, 2470 (2000).
[4] E. E. Aubanel, J. M. Gauthier, and A. D. Bandrauk, Phys. Rev. A **48**, 2145 (1993).
[5] K. Codling, L. J. Fransinski, and P. A. Hatherly, J. Phys. B: At. Mol. Opt. Phys. **22**, L321 (1995).
[6] M. Ivanov, T. Seideman, P. Corkum, F. Ilkov, and P.Dietrich, Phys. Rev. A **54**, 1541 (1996).
[7] D. Mathur and F. A. Rajgara, J. Chem. Phys. **120**, 5616 (2004).
[8] F. Legare *et al.*, Phys. Rev. A **72**, 052717 (2005).
[9] L. Zandee and R. B. Bernstein, J. Chem. Phys. **71**, 1359 (1979).
[10] C. Cornaggia, Phys. Rev. A **54**, R2555 (1996).
[11] M. Krishnamurthy, F. A. Rajgara, and D. Mathur, J. Chem. Phys. **121**, 9765 (2004).
[12] W. Fu, W. E. Schmid, and S. A. Trushin, Chem. Phys. **316**, 225 (2005).
[13] A. N. Markevitch, D. A. Romanov, S. M. Smith, and R. J. Levis, Phys. Rev. Lett. **96**, 163002 (2006).
[14] E. Baldit, S. Saugout, and C. Cornaggia, Phys. Rev. A **71**, 021403 (2005).
[15] A. Assion, T. Baumert, U. Weichmann, and G. Gerber, Phys. Rev. Lett. **86**, 5695 (2001).
[16] H. Hasegawa, A. Hishikawa, and K. Yamanouchi, Chem. Phys. Lett. **349**, 57 (2001).
[17] A. Hishikawa, H. Hasegawa, and K. Yamanouchi, Chem. Phys. Lett. **361**, 345 (2002).
[18] K. Yamanouchi, S. L. Chin, P. Agostini, and G. Ferrante (Eds.), *Progress in Ultrafast Intense Laser Science III-VIII*, Springer, Berlin, Heidelberg, 2008-2012.
[19] A. Hishikawa, A. Iwamae, and K. Yamanouchi, Phys. Rev. Lett. **83**, 1127 (1999).
[20] A. Iwasaki, A. Hishikawa, and K. Yamanouchi, Chem. Phys. Lett. **346**, 379 (2001).
[21] Y. Furukawa, K. Hoshina, and K. Yamanouchi, H. Nakano, Chem. Phys. Lett. **414**, 117 (2005).
[22] T. Okino *et al.*, Chem. Phys. Lett. **419**, 223 (2006).
[23] H. F. Schaefer III, Acc. Chem. Res. **12**, 288 (1979).
[24] Y. Wakatsuki, H. Yamazaki, N. Kumegawa, T. Satoh, and J. Y. Satoh, J. Am. Chem. Soc. **113**, 9604 (1991).
[25] A. M. Mebel, E. W. G. Diau, M. C. Lin, and K. Morokuma, J. Am. Chem. Soc. **118**, 9759 (1996).
[26] A. Hishikawa, H. Hasegawa, and K. Yamanouchi, J. Electron Spectrosc. Relat. Phenom. **141**, 195 (2004).
[27] H. L. Xu, T. Okino, and K. Yamanouchi, J. Chem. Phys. **131**, 151102 (2009).
[28] A. Hishiwa, H. Hasegawa, and K. Yamanouchi, Phys. Scr. **T110**, 108 (2004).
[29] K. Hoshina, Y. Furukawa, T. Okino, and K. Yamanouch, J. Chem. Phys. **129**, 104302 (2008).
[30] H. L. Xu, T. Okino, and K. Yamanouchi, Chem. Phys. Lett. **469**, 255 (2009).

[31] H. L. Xu, T. Okino and K. Yamanouchi, Appl. Phys. A **104**, 941 (2011).
[32] H. L. Xu *et al.*, Chem. Phys. Lett. **484**, 119 (2010).
[33] H. L. Xu *et al.*, Phys. Chem. Chem. Phys. **12**, 12939 (2010).
[34] S. Roither *et al.*, Phys. Rev. Lett. **106**, 163001 (2011).
[35] L. Zhang *et al.*, J. Phys. B: At. Mol. Opt. Phys. **45**, 085603 (2012).
[36] A. Hishikawa, A. Matsuda, E. J. Takahashi, and M. Fushitani, J. Chem. Phys. **128**, 084302 (2008).
[37] A. Matsuda, M. Fushitani, E. J. Takahashi, and A. Hishikawa, Phys. Chem. Chem. Phys. **13**, 8697 (2011).
[38] T. Okino, A. Watanabe, H. L. Xu, and K. Yamanouchi, Phys. Chem. Chem. Phys. **14**, 4230 (2012).
[39] T. Okino, A. Watanabe, H. L. Xu, and K. Yamanouchi, Phys. Chem. Chem. Phys. **14**, 10640 (2012).
[40] T. Okino *et al.*, Chem. Phys. Lett. **423**, 220 (2006).
[41] P. Liu *et al.*, Chem. Phys. Lett. **423**, 187 (2006).
[42] T. Okino *et al.*, J. Phys. B: At. Mol. Opt. Phys. **39**, S515 (2006).
[43] R. Itakura, P. Liu, Y. Furukawa, T. Okino, and K. Yamanouchi, J. Chem. Phys. **127**, 104306 (2007).
[44] R. K. Kushawaha and B. Bapat, Chem. Phys. Lett. **463**, 42 (2008).
[45] A. Matsuda, M. Fushitani, R. D. Thomas, V. Zhaunerchyk, and A. Hishikawa, J. Phys. Chem. A **113**, 2254 (2009).
[46] A. S. Alnaser *et al.*, J. Phys. B: At. Mol. Opt. Phys. **39**, S485 (2006).
[47] H. L. Xu *et al.*, J. Chem. Phys. **133**, 071103 (2010).
[48] E. Skovsen, M. Machholm, T. Ejdrup, J. Thøgersen, and H. Stapelfeldt, Phys. Rev. Lett. **89**, 133004 (2002).
[49] A. Hishikawa, M. Ueyama, and K. Yamanouchi, J. Chem. Phys. **122**, 151104 (2005).
[50] K .M. Ervin, J. Ho, and W. C. Lineberger, J. Chem. Phys. **91**, 5974 (1989)
[51] M. P. Jacobson, R. W. Field, J. Phys. Chem. A **104**, 3073 (2000).
[52] A. Hishikawa, A. Matsuda, M. Fushitani, and E. J. Takahashi, Phys. Rev. Lett. **99**, 258302 (2007).
[53] Y. H. Jiang *et al.*, Phys. Rev. Lett. **105**, 263002 (2010).
[54] H. Yazawa *et al.*, Appl. Phys. B **98**, 275 (2010).
[55] X. Xie *et al.*, Phys. Rev. Lett. **109**, 243001 (2012).
[56] H. L. Xu *et al.*, J. Phys. Chem. A **116**, 2686 (2012).
[57] A. T. J. B. Eppink, and D. H. Parker, Rev. Sci. Instrum. **68**, 3477 (1997).
[58] Z. Vager, D. Zajfman, T. Graber, and E. P. Kanter, Phys. Rev.Lett. **71**, 4319 (1993).
[59] J. Ullrich *et al.*, J. Phys. B: At. Mol. Opt. Phys. **30**, 2917 (1997).
[60] R. Dörner *et al.*, Phys. Rep. **330**, 95 (2000).
[61] RoentDek Handels GmbH. MCP Delay-Line Detector Manual.
[62] T. Weber *et al.*, Nature, **405**, 658 (2000).
[63] B. Witzel, N. A. Papadogiannis, and D. Charalambidis, Phys. Rev. Lett. **85**, 2268 (2000).
[64] R. Lafon *et al.*, Phys. Rev. Lett. **86**, 2762 (2001).
[65] G. Tejeda, B. Maté, J. M. Fernández-Sánchez, and S. Montero. Phys. Rev. Lett. **76**, 34 (1996).
[66] T. Osipov *et al.*, J. Mod. Optic. **52**, 439 (2005).
[67] S. Bubin *et al.*, Phys. Rev. A **86**, 043407 (2012).
[68] C. Wang *et al.*, Chem. Phys. Lett. **496**, 32 (2010).
[69] R. Itakura and K. Yamanouchi, J. Chem. Phys. **119**, 22 (2003).
[70] R. J. Levis, G. M. Menkir, and H. Rabitz, Science **292**, 709 (2001).

[71] B. J. Sussman, D. Townsend, M. Y. Ivanov, and A. Stolow, Science **314**, 278 (2006).
[72] H. Niikura, D. M. Villeneuve, and P. B. Corkum, Phys. Rev. A **73**, 021402 (2006).
[73] F. A. Rajgara, A. K. Dharmadhikari, D. Mathur, and C. P. Safvan, J. Chem. Phys. **130**, 231104 (2009).